Accurate Radiation-Pattern Measurements in a Time-Reversal Electromagnetic Chamber

Andrea Cozza, Abdelbassir Abou-El-Aileh

Accurate Radiation Pattern Measurements in a Time-Reversal Electromagnetic Chamber

Andrea Cozza, Ph.D.
Département de Recherche en Electromagnétisme, SUPELEC, 3 rue Joliot-Curie, 91192 Gif sur Yvette, France

Abd el-Bassir Abou el-Aileh
Université Libanaise, Faculté de Génie I, El Kobbeh, Tripoli, Lebanon

ABSTRACT

In a recent paper [1], we have introduced the concept of the Time-Reversal Electromagnetic Chamber (TREC), a new facility for creating coherent wave-fronts within a reverberation chamber. This facility, based on the use of time-reversal techniques in a reverberating environment, is here shown to be also a useful tool for the characterization of the field radiated by an antenna under test (AUT). The TREC is proven to be capable of providing real-time measurements, with an accuracy typically better than 1 dB over the main lobes, while using a limited number of static probe antennas. This performance is made possible by taking advantage of the reflections over the chamber's walls, in order to gain access to the field radiated along all the directions, with no need to mechanically displace the probes, or to have a full range of electronically switched ones. A 2D numerical validation supports this approach, proving that the proposed procedure allows the retrieval of the free-space radiation pattern of the AUT.

Keywords: Radiation Pattern Measurement, Time Reversal, Reverberation Chamber, Real Time Measurement, Time Domain.

1. Introduction

Historically, facilities for the characterization of antenna radiation can roughly be divided into two classes, one based on the mechanical displacement of one single probe [2, 3], the second using electronic switching of an array of probes in order to speed up the measurement [4]. This classification holds for both near and far-field facilities. According to the industrial context of utilisation, the two systems are interesting solutions: indeed, the electronic switching configuration is by far more complex and expensive, and its use is justified only in case of need for fast measurements. Being both based on the use of anechoic chambers, in order to have the antenna under test (AUT) radiation measured along a given direction, the probe must be aligned along it. Hence, the need for a fine mesh of sample positions for characterizing the AUT.

In this paper, we propose a change of paradigm, by advocating a reverberation chamber (RC) as a counter intuitively simpler environment for antenna testing. Although apparently hardly usable for such a purpose, due to the high-echo content of any signal measured in it, we provide a procedure that allows de-embedding the actual free-space radiation pattern (RP) of the AUT. Among its several interesting features, this solution allows carrying out a complete characterization of the AUT radiation with no need to have the probes aligned to the directions of interest. This is basically due to having exploited the reflections over the cavity walls for accessing several directions at the same time (see Fig. 1). For the same reason, the number of probes required can be reduces, while maintaining a level of accuracy below 1 dB around the RP maxima. These advantages come with a price tag, since the cavity needs to be characterized experimentally before being able to retrieve the antenna RP in free-space, thus making this solution not suitable for one-time antenna characterizations.

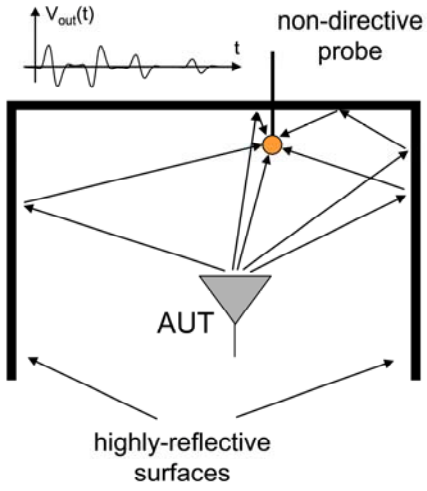

Figure 1 - A graphical explanation of how the signals received by a probe in a reverberation chamber contain information about the radiation pattern of the AUT along several directions.

2. The Time-Reversal Electromagnetic Chamber

A Time-Reversal Electromagnetic Chamber (TREC) is a facility capable of generating coherent wave-fronts inside an RC [1]. It basically exploits the properties of time reversal techniques, by ideally reversing the time-evolution of a field distribution originally generated by a given source of radiation [7]. As shown in Fig. 2, a TREC is constituted by an RC, where an array of M probe antennas are installed, generally near its walls; they will be referred to as the time-reversal mirror (TRM) antennas. These are the only antennas actively participating at the measurement with this setup. Conversely, a second array of probes is distributed at the centre of the TREC, over a usually closed surface. This second group is constituted by ideal elementary dipoles, employed as E field probes. In order to simplify the description of our technique, we will consider these probes to be physically present in the RC, though in practice they will be used only during the characterization phase, as discussed in Section 5.

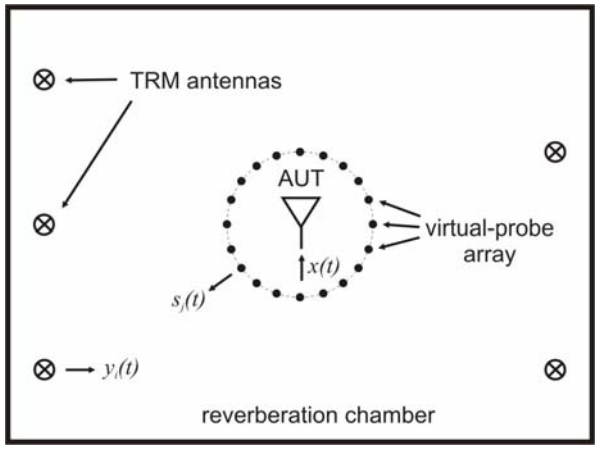

Figure 2 - Synoptic of the TREC system and the fundamental signals involved in its use.

The virtual-probe array has a fundamental role, since, it allows characterizing the transmission of energy between the TRM antennas and the region of space where a device under test (DUT) is considered for EMC purposes. The procedure introduced in [1] allows to define time-domain signals $y_i(t)$ to be applied to each of the TRM antennas in order to have them generating a coherent pulsed wave-front propagating and focusing towards the DUT, along any direction, without any need to mechanically move the TRM antennas around the DUT. This remarkable result is made possible by exploiting the reflections over the walls of the cavity, thus allowing to access the DUT along an ideally continuous range of directions.

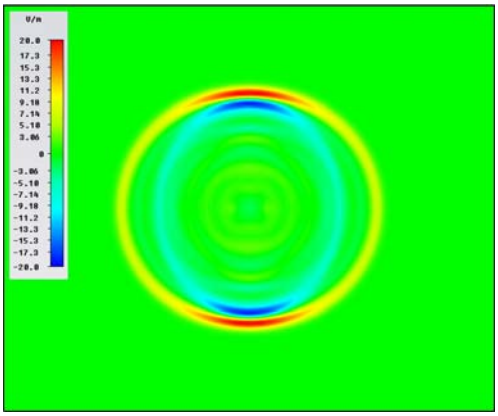

(a)

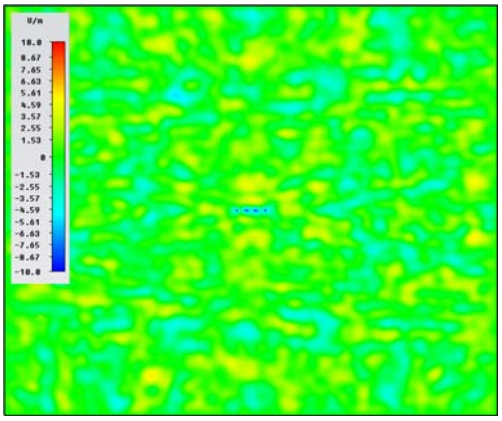

(b)

Figure 3 - Field topography within a simulated 2D RC, (a) during the time-window where propagation is still in free-space and (b) during the late-time response dominating the actual measurements.

In this paper, we prove that this technique can also be applied to the measurement of antenna RPs, and that this comes with a number of interesting features. Before going further, we need to recall some major results from time-reversal theory. It has been shown in [5, 6] that given a source of radiation in a resonant cavity, excited by a pulsed signal, and a collection of transducers acting as a TRM, the signals received by the transducers can be used for transmitting back on the former source a pulse that is very close to the original one. The ability of creating coherent transmission in a cavity was extended from a point-to-point configuration to coherent wave-fronts in [1], by introducing the idea of a virtual-array "wrapped" around a test region. Now, by considering the source of radiation to be an AUT, these precedents imply that the signals received by the TRM antennas could be used for recreating the field radiated by the AUT in the first place, but time reversed. For the sake of RP measurements, the idea of applying these signals is actually not useful; but if we knew how to relate the signals received over the TRM antennas

to the field topography over the region of space over which RP measurements are usually taken, we could recreate the field topography radiated by the antenna.

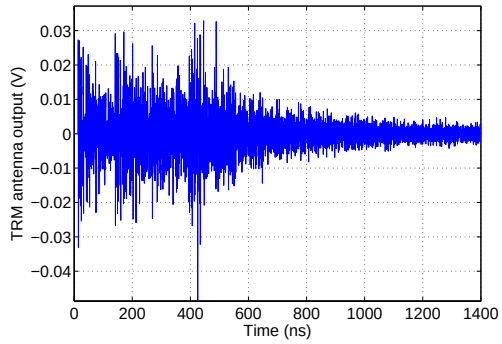

(a)

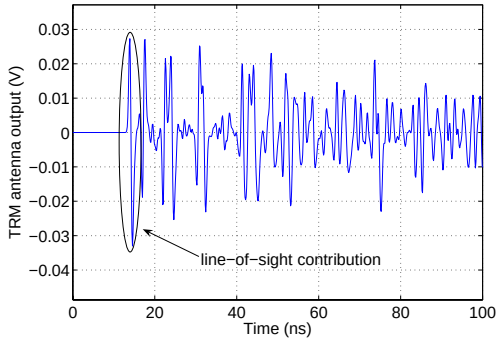

(b)

Figure 4 - Time-domain signals received by a TRM probe: (a) the typical decay of RCs, setting the minimum time needed for each measurement and (b) a zoom over the early-time response, showing the negligible impact of the line-of-sight contribution (first doublet).

The missing link for transforming this idea into an RP measurement facility is derived in the next Section. Although this technique can be straightforwardly applied to a full 3D configuration, we will limit for the scope of this paper to a 2D case. We stress the fact that preliminary experimental and numerical results show that it is possible to address the polarization of the field even with linearly polarized TRM antennas [11], with no need to rotate them as in anechoic chambers, thanks to the depolarization properties of RCs [10].

Before detailing the de-embedding procedure, we should point out some important aspects of measurements in a TREC. Fig. 3(a) shows the field topography generated by an AUT excited by a pulsed signal; during a short time-window, propagation is still as in a free-space environment, as the field radiated by the AUT has not yet interacted with the RC walls. This fact is fundamental, as the procedure detailed in Section 3 is based on this phenomenon: as long as the spatial support of the pulse is contained within the actual size of the RC, the de-embedding procedure allows to simulate a free-space environment within it. But the actual measurements are performed by the TRM antennas, and during an interval of time long enough for taking advantages of reverberations. This implies that the typical field topography will be like in Fig. 3(b): the way a TREC operates is indeed very different from the way an anechoic chamber works. This can be further asserted by taking a look at the signals received at the TRM antennas, presented in Fig. 4: Fig. 4(b) shows the line-of-sight contribution coming from the free-space radiation of the AUT; it is clear that it has a negligible contribution to the overall signal, as it is rather dominated by reflections coming from many other directions at the same time. Apart being the reason why less field probes can be used in a TREC, this also explains the fact that these signals take longer to extinguish than in free-space. This notwithstanding, recalling the physical meaning of these longer signals implies that there is no need to acquire them entirely, as they are largely redundant, being replicas of the same fundamental information, i.e., the RP of the AUT.

3. Radiation pattern retrieval

Let us consider a test signal $x(t)$ applied to the AUT. Its choice depends on its spectral content, as it is intended for soliciting the response of the AUT over a given frequency range $F = [f_1 , f_2]$. Nevertheless, an infinity of signals sharing the same spectral content can be considered. The best choice for the purpose we have set is to have it pulse-like and with the smallest time-domain support. This requirement is dictated by the fact that the propagation inside an RC can be assimilated to free-space as long as the pulsed EM field excited by the antenna does not interact with the cavity walls. Free-space propagation occurs over a short time-window lasting $T = d/(2\ c_0)$, where d is the shortest lateral dimension of the RC and c_0 is the speed of light in air. In order to retrieve the free-space radiation, it is necessary that the pulsed field radiated by the AUT has a support smaller than T. During this time-window, the virtual probes would receive the signals $s_i(t)$ that are the basis for any free-space antenna measurement procedure. Therefore, the positions of the virtual probes need to be designed as for a classic free-space facility, be it in the near- of far-field region.

As the field radiated by the AUT reaches the TRM antennas, signals $y_i(t)$ will be received on them. If we were to apply the classical time-reversal procedure [7], exciting the TRM antennas with the signals $y_i(-t)$ would lead to signals $\hat{s}_j(-t)$ measured over the virtual probes. These signals are a close replica of the signals $s_j(-t)$ [5, 6]. Let us now assume to know the pulse responses $h_{ij}(t)$ characterizing the transmission channel between the i-th TRM antenna and the j-th probe of the virtual-probe array. In this case, we can state that:

$$\hat{s}_j(t) = \sum_{i=1}^{M} y_i(-t) * h_{ij}(t) \quad , \tag{1}$$

so that as $\hat{s}_j(-t) \approx s_j(t)$, equation (1) provides a way of directly linking the signals measured on the TRM antennas to the wished ones around the AUT, at the virtual probes locations. Clearly, there is no need to actually apply the $y_i(t)$ signals to the TRM antennas, as the virtual-probe outputs can be computed as a post-processing procedure.
Applying Fourier transform to (1), yields:

$$\hat{S}_j(f) = \sum_{i=1}^{M} Y_i^*(f)\, H_{ij}(f) \quad . \tag{2}$$

These results highlight the fundamental importance of the transfer functions $H_{ij}(f)$, since acceding to them would allow providing an estimate of the field radiated near the AUT, while carrying out the actual measurement far from it and with no need for linking the TRM antenna positions and those of the virtual probes. The measurement of $h_{ij}(t)$ is the topic of Section 5. The analysis leading to (2) can be pushed further, linking the actual signals $S_j(f)$ to the estimated ones $\hat{S}_j(f)$.

To this end, we invoke Huygens principle, recalling that the signals $Y_i(f)$ can be expressed as the superposition of the contributions coming from each elementary source $S_j(f)$: Organizing the signals into column vectors, and the transfer

$$Y_i(f) = \sum_{i=1}^{N} s_j(f)\, H_{ij}(f) \quad . \tag{3}$$

functions into the channel matrix **H**, we get:

$$\hat{\mathbf{S}}^* = \mathbf{H}^H \mathbf{H}\, \mathbf{S} = \mathbf{K}\, \mathbf{S} \quad , \tag{4}$$

where the apex H stands for the Hermitian operator.
This result states that in order to have a good estimate of the field radiated by the AUT, matrix **K** needs to have a dominant main diagonal, with the value of its elements as close as possible. A complete analysis of how the properties of the **K** matrix are linked to the spatial correlation in an RC is unfortunately unfeasible in the present context, since it would take much space. Nevertheless, it can be summed up considering two issues: 1) the correlation between the TRM antennas and 2) that between the virtual probes. The TRM antennas need to be ideally uncorrelated, in order to have each one providing new degrees of freedom, and thus an improvement in the field retrieval algorithm (see Section 7). To this end, it is necessary to ensure a minimum distance of half the wavelength at the minimum frequency f_l [8]. Conversely, this requirement is not necessary for the ideal probes, since as frequency decreases and the outputs of the ideal probes start to be correlated, the maximum distance needed for computing the far-field of the AUT increases. This means that adjacent ideal probes will indeed be correlated, but it is no more necessary to consider the output of each probe, since the actual Shannon sampling distance requires a decimation of the virtual-probe array. It would rather be better to consider a sort of a sliding spatial average. This operation is implicitly accomplished by the harmonic filtering exposed in the next Section.
Signals measured in an RC are affected by long transients. Nevertheless, it was shown that the time-reversal technique attains its maximum performance after a time approximately equal to the modal density of the cavity [5]. For the system considered in Section 6, this happens after about 600 ns; for real-life RCs, a few score micro-seconds are necessary. This also set the duration of any measurement in this TREC, which is thus very fast, not requiring any additional mechanical movement.
A last important point is that since time-reversal approximates the entire propagation of the field radiated by the antenna, and this being strongly affected by the presence of reflective walls, signals $\hat{s}_j(t)$ will also contain a broad range of echoes, and not just the pulse radiated by the AUT during the free-space time window. It is thus necessary to apply a gating function to the $\hat{s}_j(t)$, hence the reason for the requirement of having the pulse radiated by the antenna to be sufficiently isolated from the first echoes. Due to this constraint, the use of the proposed procedure can be critical as soon as the AUT becomes resonant and poorly efficient, since in this case it would radiate long undamped harmonics that could exceed the free-space time window, so that it would be impossible to separate the direct radiation from the first echoes coming from the walls
.

4. Angular harmonic filtering

It will be shown in Section 6 that the field distribution retrieved by means of this approach is characterized by fast angular variations that are not physical for far-field radiation. Since time reversal is fundamentally a propagation operator, no reactive component of the originally radiated field could be generated, so that these variations must be related to an imperfect reconstruction (see Section 7). An effective way of filtering these errors out of the estimated RP is to apply the procedure described in [8], i.e., limiting the Fourier series expansion of the RP to its first N terms, with N given by

where R is the radius of the smallest circle containing the

$$N = \lceil kR \rceil \quad , \tag{5}$$

AUT, and k is the wave-number. These N terms correspond to the cylindrical harmonics that would indeed propagate in free-space at a given frequency. Although for a different reason, this truncation is to be applied also to the RP derived from the $s_i(t)$ measured over the virtual-probe array during the free-space time window: in this case it is needed for filtering the reactive components of the field excited by

the AUT, since at low frequencies the probes will not meet the far-field distance condition.

5. Medium characterization

We have shown in Section 3 the central role played by the channel matrix **H**. The application of the proposed method is conditioned by the availability of an accurate estimate of this matrix. Since the virtual probes are not intended for emission, but just for sampling the E field, one way of measuring the $H_{ij}(f)$ functions is to feed each TRM antenna with a test signal $x(t)$, while measuring the signals $p_i(t)$ received at the virtual probes locations. The transfer functions $H_{ij}(f)$ can thus be computed by means of a direct deconvolution

$$H_{ij}(f) = \frac{P_j(f)}{X(f)} \quad , \qquad (6)$$

having applied $x(t)$ to the i-th TRM antenna. Equation (6) is well-defined as long as $X(f)$ has no zero-crossings: this is the case, e.g., for Gaussian pulses and, clearly, sine-wave signals used for harmonic excitation in frequency domain. The main difficulty in obtaining the channel matrix is clearly the need for an array of ideal probes. This scenario can be very well approximated by using phase-preserving all-optical E-field probes. Rather than deploying an actual array of such probes, the negligible scattering they provide means that the probe can be moved around the AUT, while collecting the $H_{ij}(f)$. Clearly, this is the same scenario underlying any near-field radiation-pattern measurement, so that one could ask whether the proposed method is sensible. The key for understanding its interest is that as long as the channel matrix **H** stays unchanged, it needs not be characterized again. This rules out using the TREC-based method for one-time blind characterizations; conversely, it is an interesting alternative to existing facilities in at least two real-life scenarios: 1) mass-produced radiating equipments, where the field they radiate may change, due to manufacturing tolerances/faults, while maintaining exactly the same mechanical structure and 2) large phased-arrays where the number of radiation configurations can be quite high, leading to a long characterization time. These two configurations share a common feature, i.e., the presence of a static mechanical configuration, while the field radiated by the AUT can change. Indeed, the use of the TREC requires dissociating the free-space radiation of the AUT and the propagation inside it.

A final consideration about the channel matrix is necessary: recalling the results from RC theory, the sensitivity of any transfer function to mechanical displacements is related to their electrical distance. Indeed, the spatial correlation stays high as long as the displacements involve distances shorter than $\lambda/8$ [8].

6. Numerical results

The proposed method was investigated by means of numerical simulations, carried out in time domain thanks to CST's Microwave Studio. The cavity was a quasi-2D one, with transversal dimensions of 8x6.4 m^2, and a thickness of 15 cm, hence enforcing the existence only of purely

transversal resonant modes up to 1 GHz. The fact of having the two main walls made out of a perfect electric conductor, and at a distance that is electrically small over the entire frequency range, implies that the E field is almost scalar and propagating over a planar surface. This configuration has allowed the introduction of the simplified model presented in Section 3.

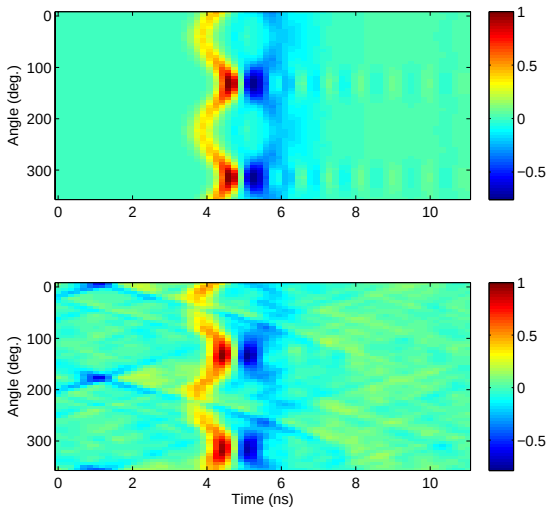

Figure 5 – Time-domain reconstruction of the E field radiated by the AUT during the free-space time window. The two sets of signals have been normalized to their peak value. These results refer to the use of the 12 TRM antennas.

Twelve TRM antennas were placed along two facing walls, six by side, in a way similar to that of Fig. 2. The distance between adjacent TRM antennas was fixed at about 1 m, which ensures that their responses are well uncorrelated down to 100 MHz. The distance between the TRM antennas and the walls was set at 30 cm; the only requirement is that the walls do not short-circuit too much the antennas. Half-wavelength dipoles were used, resonating at 1 GHz. A virtual-probe array made up of 64 ideal probes was considered, uniformly distributed over a circumference 2 m wide in diameter. Shannon sampling theorem for a cylindrical configuration requires at least 18 probes up to 1.5 GHz in free-space for propagative field components [12].

The AUT was a four-element uniform linear array constituted by the same dipoles as the TRM antennas. The axis of the array was tilted of a 45-degree angle in order to avoid long propagation paths in the case of directive broadside radiation away from the TRM antennas. The array was chosen as an AUT since it allows checking one of the most important features of the TREC-based system, i.e., that as long as the mechanical/propagation configuration of the cavity-AUT system are unmodified, the same channel matrix **H** can be applied. To this end, the array was fed with several phase-shifts, in order to tilt the main radiation lobe. After applying the characterization procedure detailed in Section 5, the AUT was finally excited with a base-band Gaussian pulse, covering frequencies up to 1.5 GHz, and the corresponding TRM signals recorded. Time-domain signals over the virtual-probe array was retrieved by means of the technique proposed in Section 3. An example of these results is shown, in time domain, for a broadside radiation, in Fig. 5. Indeed, the pulsed field radiated by the AUT is well identified, even though fewer TRM antennas are used than the number of probes that would be necessary in a near-field free-space setup. Fig. 5 shows that the reconstructed field is affected by spurious propagation traces, due to the limited number of resonant modes involved in the lower frequency range. The obtained results prove that the free-space assumption holds, since the first echoes are seen over the probe array only after 23 ns (not shown), so that a gating over the first 11 ns allows removing them. Although the right-end of the gating interval can be freely placed between 7 and 23 ns, the choice of the left-end is more critical. This is due to the fact that the signals reconstructed through time-reversal are related to a wave-front very similar to the one originally emitted by the AUT, but moving back towards it. Hence, the first 3 ns deal with the field that would be scattered back by the AUT and measured by the virtual-probe array. This contribution is thus unwanted and must be accurately removed.

By Fourier-transforming the time-domain results, the field radiated by the AUT under a CW excitation can be retrieved. Fig. 7 presents a few RPs obtained after applying the angular harmonic filtering described in Section 4. Two feeding configurations were considered, for a tilt angle of zero degrees (with respect to the broadside direction) and 45 degrees. As a matter of fact, the free-space RPs are very well characterized, presenting a maximum error below 1 dB over the first 10 dB range. As expected in any retrieval procedure, the most critical parts are the nulls.

These results prove that indeed, if the AUT is to be tested for several radiation configurations, while maintaining a static mechanical setup, the proposed procedure is indeed interesting, allowing a full characterization with less signals to be measured with respect to an anechoic environment.

7. On the quality of the reconstruction

The concept of quality can be formalized by recalling that the reconstructed field can be regarded as given by the superposition of a coherent part, i.e., the original signal to be estimated and an incoherent one, i.e., the residual noise in the reconstruction. The quality is thus given by the square of the ratio of the amplitude of the coherent part and the incoherent one [5, 6]. Interestingly, it can be assimilated to a signal to noise ratio.

The accuracy of the reconstruction can be shown to depend on two issues, the number of resonant modes excited in the

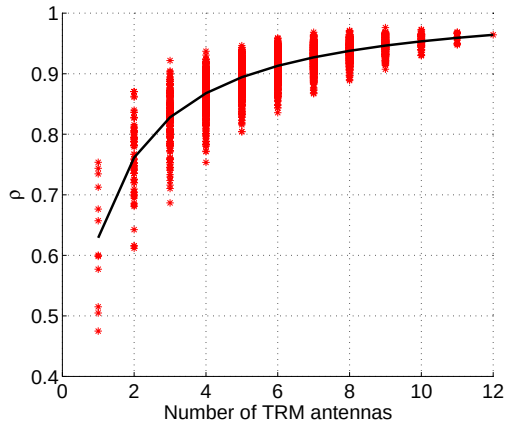

(a)

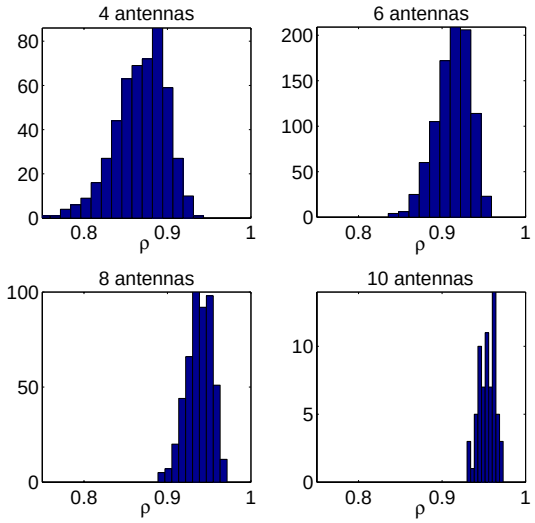

(b)

cavity and the number of TRM antennas. The former is the most important one, since it does not lend itself to modifications introduced by the designer. Indeed, the resonant behaviour of the cavity is a function of the frequency, and it is strongly related to the physical dimensions of the cavity as well as the conductivity of the materials involved; in other words, the quality factor of the cavity. As long as the cavity is strongly resonant, it can be shown that the quality of the reconstruction is directly proportional to the number of modes excited over the bandwidth spanned by the test pulse $x(t)$ [6]. Since this goes as the square of the frequency, the reconstruction is expected to get better at the higher-frequency end.

In order to understand how the number of TRM antennas impact the quality of the reconstruction, it is necessary to assume that their electrical distance is sufficiently high as to ensure a very low correlation between the transfer functions relating a given virtual probe to a pair of TRM antennas. Under these conditions, the contribution of each TRM antenna to the reconstructed field will be uncorrelated from the others, so that the residual incoherent noise will sum up in energy and not in amplitude, whereas the opposite will be true for the coherent part. This means that the quality of the reconstruction (the signal-to-noise ratio) grows like M.

Hence, the number of TRM antennas can be expected to play a minor role with respect to the number of resonant modes excited. Nevertheless, as the frequency decreases, the number of modes reduces, so that increasing the number of TRM antennas is a viable solution for improving the performance of the TREC-based system.

We investigated the impact of the number of antennas by computing the correlation coefficient ρ between the retrieved RP and the free-space one, in time domain, averaged over 2π steradians. This operation was carried out for all the combinations of signals received over the TRM antennas: after setting the number of TRM antennas to be used, only a subset of signals were considered in the RP retrieval, and this for all the combinations of signals picked-up from the pool of 12 TRM signals. The results of this analysis are shown in Fig. 6, where they make clear that the actual position of the TRM antennas has an impact of the quality of the reconstruction, as the correlation coefficient appears to behave according to a bell-shaped probability density function.

Figure 6 - Impact of the number of active TRM antennas on the average correlation coefficient ρ between the reconstructed RP and the original one, in time domain: (a) scatter plot (the solid line stands for the average ρ for a given number of antennas) and (b) empirical probability density functions.

In order to ensure reliable results for any positioning, the minimum number of antennas need to be increased. Considering a threshold of about 0.9 for the average ρ leads to requiring 9 antennas, as opposed to the 18 needed from Shannon theorem. No major degradation is expected passing from 12 to 9 antennas, as proven by the results in Fig. 6. These conclusions are just for a scalar configuration, but it is important to recall that it is expected to be capable of retrieving also a vector field distribution, as required for a 3D configuration. The results presented in [10, 11] imply that whereas in an anechoic environment the number of field probes would need to be doubled (two tangential components are required), the number of TRM antennas could be left unchanged. Hence, the TREC is expected to allow a fourfold reduction in the number of measurements needed with respect to an anechoic facility.

8. Conclusions and perspectives

In this paper we have proven that, against received wisdom, RCs can be an interesting alternative to anechoic chambers as facilities for accurately characterizing the RP of an AUT. A modified RC configuration was advocated, the

TREC, which among other advantages allows reducing the number of probe antennas needed for the measurement by a factor four, as well as avoiding any mechanical movement. These features are made available by the use of a theoretical procedure that allows retrieving the free-space field radiated by the AUT, thanks to the properties of time-reversal techniques. A medium characterization procedure being necessary, this technique is not suitable for one-time characterizations, but it proves to be powerful as soon as static/repetitive configurations are involved, so that the same channel matrix can be applied, leading to a strong reduction of the characterization time. Despite the present analysis focuses on a scalar 2D chamber, it can be proven that this technique can be extended to a full 3D vector configuration, without any need to consider more complex TRM antennas. These results are of course just preliminary to a full-scale validation involving a 3D TREC.

9. REFERENCES

[1] H. Moussa, A. Cozza, and M. Cauterman, "Directive wave-fronts inside a Time-Reversal Electromagnetic Chamber", IEEE Electromagnetic Compatibility Symposium, 17-21 August 2009, Austin, Texas.

[2] J.D. Kraus, *Antennas*, McGraw-Hill, Second Edition, 1988.

[3] J. Way, K. Haner, "A low-cost spherical near-field system", AMTA Symposium, 3-7 October 1994.

[4] P.O. Iversen, P. Garreau, K. Englund, E. Pasalic, O. Edvardsson, G. Engblom, "Real Time Spherical Near Field Antenna Test Range for Wireless Applications", AMTA Symposium, 4-8 October 1999, Monterey Bay, California.

[5] J. De Rosny, *Milieux réverbérants et réversibilité*, Ph.D. Thesis, Université Pierre et Marie Curie, Defended on 17 July 2000, Paris, France.

[6] A. Cozza, "Statistics of the performance of time-reversal in a lossy reverberating medium", Physical Review E, Vol. 80, November 2009.

[7] D. Cassereau and M. Fink, "Time-reversal of ultrasonic fields III : Theory of the closed time-reversal cavity", *IEEE Trans. on Ultrasonics, Ferroelectrics and Frequency Control*, Vol. 39, No. 5, 1992.

[8] D.A. Hill, J.M. Ladbury, "Spatial-correlation functions of fields and energy density in a reverberation chamber", *IEEE Trans. on Electromagnetic Compatibility*, Vol. 44, No. 1, 2002.

[9] O.M. Bucci, G. Franceschetti, "On the degrees of freedom of scattered fields", *IEEE Trans. on Antennas and Propagation*, Vol. 37, No. 7, 1989.

[10] A. Cozza, H. Moussa, "Enforcing deterministic polarisation in a reverberating environment", Electronics Letters, Vol. 45, 2009.

[11] H, Moussa, A. Cozza, M. Cauterman, "Experimental analysis of the performance of a time‐reversal electromagnetic chamber", Asia-Pacific Electromagnetic Compatibility Symposium, April 2010, Beijing.

[12] J.E. Hansen, *Spherical Near-Field Antenna Measurements*, Peter Peregrinus Ltd, 1988.

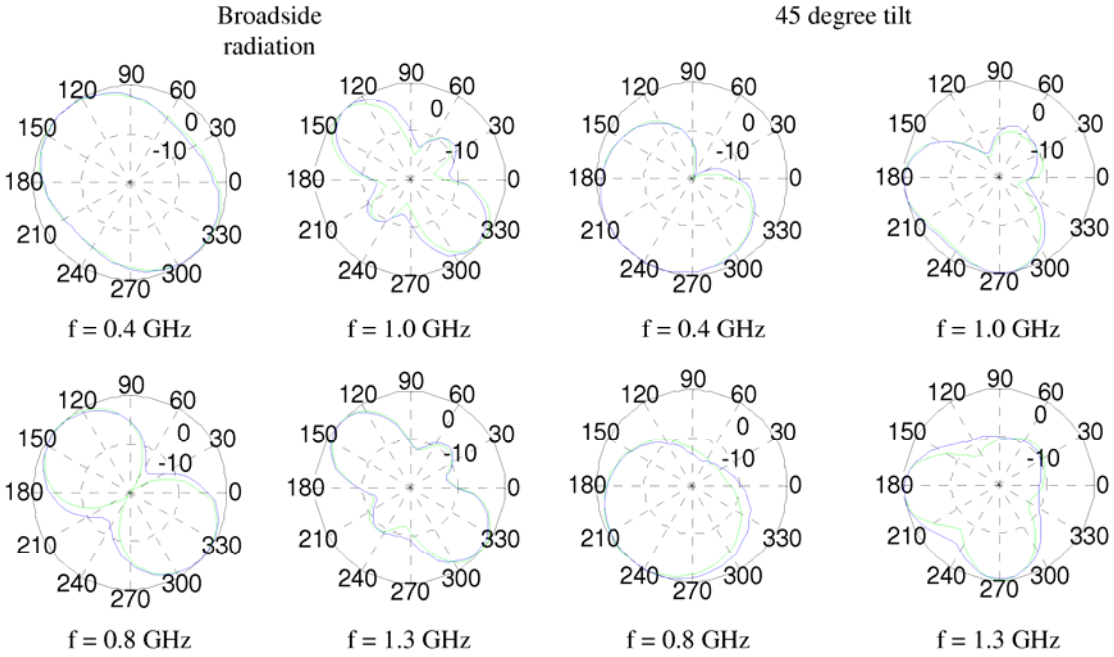

Figure 7 – Some results from the numerical validation, comparing the RPs derived from the E field as measured over the virtual probes during the free-space time window (lighter lines) and those retrieved from signals measured on the TRM antennas (darker lines). The RPs are represented on a 20 dB dynamic range. These results refer to the use of 12 TRM antennas.